4642 *Biochemistry* **2009,** *48,* 4642–4651
DOI: 10.1021/bi802171c

BIOCHEMISTRY
including biophysical chemistry & molecular biology
Article

Regulatory Autophosphorylation Sites on Protein Kinase C-δ at Threonine-141 and Threonine-295†

Vitalyi O. Rybin, Jianfen Guo, Erin Harleton, Steven J. Feinmark, and Susan F. Steinberg*

Department of Pharmacology, Columbia University, New York, New York 10032

Received November 24, 2008; Revised Manuscript Received March 19, 2009

ABSTRACT: Protein kinase C-δ (PKCδ) is a Ser/Thr kinase that regulates a wide range of cellular responses. This study identifies novel *in vitro* PKCδ autophosphorylation sites at Thr^{141} adjacent to the pseudosubstrate domain, Thr^{218} in the C1A-C1B interdomain, Ser^{295}, Ser^{302}, and Ser^{304} in the hinge region, and Ser^{503} adjacent to Thr^{505} in the activation loop. Cell-based studies show that Thr^{141} and Thr^{295} also are phosphorylated *in vivo* and that Thr^{141} phosphorylation regulates the kinetics of PKCδ downregulation in COS7 cells. *In vitro* studies implicate Thr^{141} and Thr^{295} autophosphorylation as modifications that regulate PKCδ activity. A T141D substitution markedly increases basal lipid-independent PKCδ activity; the PKCδ-T141D mutant is only slightly further stimulated *in vitro* by PMA treatment, suggesting that Thr^{141} phosphorylation relieves autoinhibitory constraints that limit PKCδ activity. Mutagenesis studies also indicate that a phosphorylation at Thr^{295} contributes to the control of PKCδ substrate specificity. We previously demonstrated that PKCδ phosphorylates the myofilament protein cardiac troponin I (cTnI) at Ser^{23}/Ser^{24} when it is allosterically activated by lipid cofactors and that the Thr^{505}/Tyr^{311}-phosphorylated form of PKCδ (that is present in assays with Src) acquires as additional activity toward cTnI-Thr^{144}. Studies reported herein show that a T505A substitution reduces PKCδ-Thr^{295} autophosphorylation and that a T295A substitution leads to a defect in Src-dependent PKCδ-Tyr^{311} phosphorylation and PKCδ-dependent cTnI-Thr^{144} phosphorylation. These results implicate PKCδ-Thr^{295} autophosphorylation as a lipid-dependent modification that links PKCδ-Thr^{505} phosphorylation to Src-dependent regulation of PKCδ catalytic function. Collectively, these studies identify novel regulatory autophosphorylations on PKCδ that serve as markers and regulators of PKCδ activity.

Protein kinase C-δ (PKCδ) is a member of the PKC family of serine/threonine kinases that sit at the crossroads of signal transduction pathways implicated in a wide range of cellular responses (*1*). PKCδ's structure consists of a highly conserved C-terminal catalytic domain (consisting of motifs required for ATP/substrate binding and catalysis) and an N-terminal regulatory domain containing tandem C1A-C1B domains that bind lipid cofactors, a C2 domain that acts as a protein−protein interaction module, and an autoinhibitory pseudosubstrate domain (a sequence lacking a serine/threonine phosphoacceptor site but otherwise resembling a PKC[1] substrate) that maintains the enzyme in an inactive conformation. Like other PKC isoforms, PKCδ is activated by growth factor receptors that promote the accumulation of lipid cofactors such as diacylglycerol (DAG) or by tumor-promoting phorbol esters such as phorbol 12-myristate 13-acetate (PMA) that anchor the enzyme in an active conformation to membranes. However, recent studies expose phosphorylation at a highly conserved threonine residue in the activation loop (Thr^{505}) as an additional component of the PKCδ activation mechanism (*2*). For most PKC isoforms, activation loop phosphorylation is a stable "priming" modification that is mediated by PDK-1 and serves (along with additional phosphorylation events at conserved turn and hydrophobic motifs in the C-terminus) to lock the enzyme in a mature catalytically competent conformation, poised to be allosterically activated by lipid cofactors (*3*). In contrast, PKCδ is catalytically active even without Thr^{505} phosphorylation. Rather, PKCδ-Thr^{505} phosphorylation has emerged as a dynamically regulated autocatalytic reaction that "fine-tunes" PKCδ's catalytic function toward selected substrates (*4*).

†This work was supported by USPHS NHLBI Grant HL 77860 and TL1 RR024158 from the National Center for Research Resources (NCRR), a component of the National Institutes of Health (NIH) and NIH Roadmap for Medical Research. Its contents are solely the responsibility of the authors and do not necessarily represent the official view of the NCRR or NIH. Information on NCRR is available at http://www.ncrr.nih.gov/. Information on Re-engineering the Clinical Research Enterprise can be obtained from http://nihroadmap.nih.gov/clinicalresearch/overview-translational.asp.

*Address correspondence to this author. Tel: 212-305-4297. Fax: 212-305-8780. E-mail: sfs1@columbia.edu.

[1]Abbreviations: cTnI, cardiac troponin I; DAG, diacylglycerol; diC8, 1,2-dioctanoylglycerol; EGFP, enhanced green fluorescent protein; ESI-LC/MS/MS, electrospray ionization−liquid chromatography/tandem mass spectrometry; PDK-1, phosphoinositide-dependent kinase 1; PKC, protein kinase C; aPKC, atypical protein kinase C; cPKC, conventional protein kinase C; nPKC, novel protein kinase C; PKD1, protein kinase D1; PMA, phorbol 12-myristate 13-acetate; PS, phosphatidylserine; PSSA, phospho-site-specific antibody; RP-HPLC, reverse-phase high-pressure liquid chromatography.

 Published on Web 04/14/2009

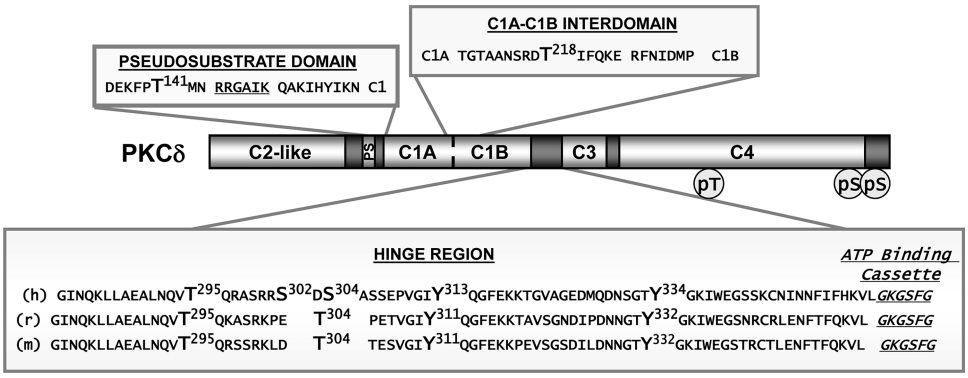

FIGURE 1: Schematic of autophosphorylation sites adjacent to the pseudosubstrate domain, in the C1A-C1B interdomain region, and in the hinge region of PKCδ. Domain structure of PKCδ with conserved (C2-like and C1A-C1B) regions in the regulatory domain and conserved (C3 and C4) regions in the catalytic domain. The PKCδ autophosphorylation sites identified in this study are located N-terminal to the pseudosubstrate (PS) domain sequence (which is underlined in the figure), in the C1A-C1B interdomain, and in the hinge region. PKCδ tyrosine phosphorylation sites at position Tyr^{155} (C-terminal to the pseudosubstrate domain sequence) and at tyrosine residues in the hinge region also are indicated. Pseudosubstrate and C1A-C1B intedomain regions of PKCδ are evolutionarily conserved; species differences in the hinge region sequences of human (h), rat (r), and mouse (m) PKCδ are provided.

While *in vitro* intramolecular autophosphorylations of brain PKC were described over 20 years ago (*5*), conventional models of PKC isoform activation do not consider a possible role for autophosphorylation reactions that regulate PKC enzyme activity. Nevertheless, an early study mapped PKC-βII autophosphorylation to Ser^{16} and Thr^{17} in the N-terminus, Thr^{314} and Thr^{324} in the hinge region, and Thr^{641} in the C-terminus (*6*). Thr^{641} resides in the turn motif, a highly conserved phosphorylation motif in all PKC isoforms. Other PKCβII autophosphorylation sites in the hinge region and N-terminus are not conserved in other PKC isoforms; since these autophosphorylation sites were not identified in subsequent studies that mapped *in vivo* PKCβII phosphorylation to Thr^{500} (the activation loop), Thr^{641} (the turn motif), and Ser^{660} (the hydrophobic motif (*7*)), N-terminal and hinge region phosphorylation sites in PKCs were largely ignored in subsequent literature. The single exception is a modeling study from the Newton laboratory which considered a possible role for PKCβII-Ser^{16}/Thr^{17} autophosphorylation as a mechanism that favors activation by lowering pseudosubstrate domain binding affinity for the catalytic pocket (*6*, *8*). Interest in PKC autophosphorylation has recently been rekindled by studies from the Parker laboratory showing that human PKCδ and PKCε autophosphorylate at sites in their variable hinge regions (*9*, *10*); autophosphorylation sites in the hinge region of human PKCδ were mapped to Ser^{299}, Ser^{302}, and Ser^{304} (Figure 1). PKCδ and PKCε autophosphorylation reactions have generally been viewed as markers of enzyme activation. The notion that hinge region autophosphorylation reactions might regulate the catalytic properties of PKCδ has never been considered.

There is recent evidence that PKCδ activity also is controlled through tyrosine phosphorylation. As many as eight highly conserved tyrosine residues in various regions of PKCδ's structure have been implicated as targets for regulatory phosphorylations. Our recent studies focused on PKCδ phosphorylation at Tyr^{311} and Tyr^{332}, residues unique to the hinge region of PKCδ that are phosphorylated *in vitro* by Src or related Src family kinases (*2*, *4*, *11*). We showed that PKCδ-Tyr^{311} phosphorylation increases *in vivo* in PMA- and H_2O_2-treated cardiomyocytes (*2*). While PKCδ phosphorylation at tyrosine residues and at the activation loop (at Thr^{505}) generally are viewed as independently regulated events, our recent experiments exposed a novel form of cross-regulation, showing that Src and PKCδ-Tyr^{311}/Tyr^{332} phosphorylation enhances PKCδ-Thr^{505} autophosphorylation (*2*). We also demonstrated that phosphorylations at Tyr^{311} and Thr^{505} cooperate to "fine-tune" PKCδ's enzymology toward cardiac troponin I (cTnI), a physiologically important PKCδ substrate in the heart (*4*). cTnI is the "inhibitory" subunit of the troponin complex that is critical for Ca^{2+}-dependent regulation of myofilament function (*12*). cTnI contains three phosphorylation clusters (Ser^{23}/Ser^{24}, Ser^{43}/Ser^{45}, and Thr^{144}) that exert distinct effects on cardiac function. We showed that (1) allosterically activated PKCδ (in assays with PS/PMA) phosphorylates cTnI at Ser^{23}/Ser^{24} and that this modification leads to depressed tension at submaximum but not maximum [Ca^{2+}] in detergent-extracted single cardiomyocytes, (2) PKCδ becomes a cTnI-Thr^{144} kinase (and phosphorylates cTnI at both Ser^{23}/Ser^{24} and Thr^{144}) and that PKCδ depresses maximum tension and cross-bridge kinetics in single detergent-extracted cardiomyocytes when it is tyrosine phosphorylated by Src, and (3) the effect of Src to convert PKCδ into a cTnI-Thr^{144} kinase is abrogated by PKCδ-Y311F or T505A substitutions (*4*). These results implicate PKCδ-Tyr^{311}/Thr^{505} phosphorylation as dynamically regulated modifications that alter PKCδ enzymology and allow for stimulus-specific control of cardiac mechanics during growth factor stimulation and oxidative stress. Studies reported herein identify additional novel PKCδ autophosphorylation sites that regulate PKCδ activity.

EXPERIMENTAL PROCEDURES

Materials. Antibodies were from the following sources: PKCδ-Thr(P)^{505}, PKCδ-Tyr(P)^{311}, troponin I-Ser(P)^{23}/Ser(P)^{24}, and anti-pTXR, Cell Signaling Technology; PKCδ, Santa Cruz Biotechnology; mouse monoclonal anti-GFP antibody 3E6, Invitrogen. Recombinant human PKCδ was from Calbiochem. The human recombinant full-length His-tagged Src enzyme, expressed in Sf9 cells and purified by sequential chromatography (purity >95% by Coomassie blue staining of the SDS−PAGE gel) was obtained from Invitrogen. Previous studies further validated the purity of this enzyme preparation, showing that (1) the kinase activity in this preparation is completely blocked by the Src inhibitor PP1 and (2) this enzyme preparation is detected as a single radioactive band corresponding to the autophosphorylated Src protein when it is subjected to *in vitro* kinase assays with [^{32}P]ATP and then run on a gel (i.e., no other enzymes/substrates are detected even with long exposures of

the gel (*4*)). PMA was from Sigma. 1,2-Dioleoyl-*sn*-glycerol was from Avanti Polar Lipids, Inc. Other chemicals were of reagent grade.

Cardiomyocyte Culture. Cardiomyocytes were isolated from hearts of 2-day-old Wistar rats by a trypsin dispersion procedure that uses a differential attachment procedure followed by irradiation to enrich for cardiomyocytes (*11*). Cells were plated on protamine sulfate-coated culture dishes at a density of 5×10^6 cells/100 mm dish and grown in MEM (Gibco, BRL) supplemented with 10% fetal calf serum for 4 days and then serum-deprived for 24 h prior to experiments.

For studies of PKCδ phosphorylation *in vivo* in cardiomyocyte cultures, cardiomyocytes were infected with an adenoviral construct that drives expression of mouse PKCδ. Two days later, the cultures were incubated for 4−5 h at 37 °C in phosphate-free MEM containing [^{32}P]orthophosphate (0.15−0.26 mCi/mL, 4 mL per dish). Cardiomyocytes were then treated for 10 min with vehicle or 5 mM H_2O_2, and experiments were terminated by aspirating the radioactive medium and rinsing culture dishes with a buffer containing 133 mM NaCl, 4.7 mM KCl, 1.8 mM $CaCl_2$, 16.5 mM dextrose, and 20 mM HEPES. Cellular proteins were harvested in homogenization buffer (20 mM Tris-HCl, pH 7.5, 0.05 mM EDTA, 0.5 mM DTT, 0.2% Triton X-100, 5 μg/mL aprotinin, 5 μg/mL leupeptin, 5 μg/mL benzamidine, 1 mM PMSF, 5 μM pepstatin A), and PKCδ was immunoprecipitated, separated from other cellular proteins by SDS−PAGE, and subjected to phosphopeptide mapping analysis.

PKCδ Mutants. pPKCδ-EGFP (pGFP-PKCδ) was obtained as a generous gift from Dr. Mary Reyland (University of Colorado Health Sciences Center, Denver, CO). The pPKCδ-EGFP construct expresses mouse PKCδ with enhanced GFP fused to its C-terminus. pPKCδT141A-EGFP, pPKCδT141D-EGFP, and pPKCδT295A-EGFP were generated by site-directed mutagenesis according to the manual for the Quick-Change site-directed mutagenesis kit (Stratagene). PKCδ expression plasmids were introduced into COS7 cells by effectene transfection reagent (Qiagen) according to the instruction manual. Cells were grown for 24 h, lysed in homogenization buffer. Cell extracts were subjected to immunoprecipitation with mouse monoclonal anti-GFP antibody 3E6 (Invitrogen).

In Vitro Kinase Assays with Recombinant Enzymes. *In vitro* kinase assays were performed with 0.032 unit (32.4 ng) of recombinant human PKCδ (Calbiochem) for assays of cTn complex phosphorylation or 0.4 unit for peptide mapping studies. Assays were performed in 80 μL of a reaction buffer containing 30 mM Tris-HCl, pH 7.5, 5 mM $MgCl_2$, 10 mM $MnCl_2$, 0.9 mM EDTA, 0.9 mM EGTA, 3 mM DTT, 0.1 mM sodium vanadate, 76 mM NaCl, 23.5% glycerol, 0.006% Brij-35, 0.023% Triton X-100, 0.04 mM phenylmethanesulfonyl fluoride, 0.2 mM benzamidine, 83 μg/mL phosphatidylserine (PS), 175 nM PMA, 4 μg of troponin complex, and [γ-^{32}P]ATP (25 μCi, 97 μM, unless indicated otherwise). Incubations were for 30 min at 30 °C in the absence or presence of Src (0.66 unit) or lipid cofactors. PS/PMA is included in assays to allosterically activate PKCδ and render it a better substrate for Src-dependent tyrosine phosphorylation (*11*).

Immunoblotting Studies. Immunoblotting was performed on cell extracts according to methods described previously or manufacturer's instructions (*11*). In each figure, each panel represents the results from a single gel (exposed for a uniform duration); detection was with enhanced chemiluminescence, and quantification was by laser scanning densitometry. All results were replicated in at least three experiments.

Peptide Mapping Studies. For peptide mapping studies, kinase reactions (see above) were stopped by adding 27 μL of 4× SDS−PAGE sample buffer. Proteins were separated by SDS−PAGE and transferred to nitrocellulose, and the band corresponding to PKCδ was excised from the membrane, cut into small pieces, and treated for 30 min at 37 °C with polyvinylpyrrolidone (0.5%, w/v) in acetic acid (100 mM), followed by five water washes (to remove the acid) and a 10 min incubation at room temperature in the dark with 100 mM iodoacetate to carboxymethylate PKCδ. Membrane pieces were then washed three times with water and twice with 50 mM ammonium bicarbonate and incubated overnight at 37 °C in 60 μL of a buffer containing 42 mM ammonium bicarbonate, 17 μM HCl, and 10 μg of sequencing grade trypsin. Digested peptides were eluted from the membrane by sonication and lyophilized, and the residue was reconstituted in 0.1% trifluoroacetic acid and fractionated by RP-HPLC on a Vydac semimicro C_{18} column (2.1 × 250 mm). Peptides were eluted with a linear gradient from 0.1% trifluoroacetic acid in water to 0.1% trifluoroacetic acid in acetonitrile over 140 min at a flow rate of 1 mL/min. The eluant was monitored at 220 nm, and fractions were collected every 30 s for Cherenkov counting. Fractions containing radioactivity were subjected to LC-MS/MS analysis on a Micromass Q-Tof hybrid quadrupole/time-of-flight mass spectrometer with a nanoelectrospray source. Capillary voltage was set at 1.8 kV and cone voltage 32 V; collision energy was set according to mass and charge of the ion, from 14 to 50 eV. Chromatography was performed on an LC Packings HPLC with a C18 PepMap column using a linear acetonitrile gradient with flow rate of 200 nL/ min. Raw data files were processed using the MassLynx version 4.0 ProteinLynx software with the MaxEnt 3 algorithm. Phosphorylated peptides were verified by manual inspection of MS/MS spectra.

RESULTS

Phosphopeptide Mapping Studies Identify PKCδ Autophosphorylation at Thr^{141}, Thr^{218}, Thr^{295}, Ser^{302}, Ser^{304}, and Ser^{503}. Recombinant PKCδ (human sequence) was phosphorylated *in vitro* in buffers containing [γ-^{32}P]ATP and PS/PMA. Since these studies were performed as part of an ongoing effort to identify sites for PKCδ phosphorylation by Src, assays were performed without and with active Src. Radiolabeled PKCδ from the *in vitro* kinase assays was purified by SDS−PAGE, blotted to nitrocellulose, excised from the membrane, and then subjected to digestion with trypsin and fractionation by reverse-phase HPLC. Figure 2 shows that RP-HPLC chromatograms of phosphopeptide fragments derived from *in vitro* kinase assays with PKCδ, Src, and [γ-^{32}P]ATP contained two distinct radioactive peaks that are not present in the chromatograms from kinase assays with PKCδ alone (peaks 1 and 4). Sequencing of peptides in these peaks by electrospray ionization (ESI) LC/MS/MS analysis identified phospho-Tyr^{313}- and phospho-Tyr^{334}-containing fragments (corresponding to phospho-Tyr^{311} and phospho-Tyr^{332} in rodent PKCδ; see Figure 1). Peptides containing Tyr^{64} and Tyr^{52} also were recovered in peak 4; while these tyrosine residues also have been identified as sites for regulatory phosphorylation, these peptide fragments were not phosphorylated. Sequencing of these and other peaks by ESI-LC/MS/MS analysis achieved ~40% coverage of the

PKCδ sequence and identified six novel sites for PKCδ autophosphorylation: (*1*) Peak 2 contains a peptide fragment that is phosphorylated at Thr[218]; this residue resides in a phosphorylation motif that is evolutionarily conserved in the C1A-C1B interdomain regions of PKCδ and PKCθ but not other PKC isoforms (*13*). (2) Peak 3 contains a peptide fragment that is phosphorylated at Thr[141]. The Thr[141] phosphorylation motif is conserved in PKCη but not PKCθ or other PKC isoforms. Of note, Thr[141] is positioned N-terminal to the pseudosubstrate domain of PKCδ, similar to the position of Ser[16]Thr[17] relative to the pseudosubstrate domain ($_{22}$RKGALR[27]) of PKCβII. These results suggest that PKCδ-Thr[141] and PKCβII-Ser[16]Thr[17] autophosphorylation reactions might subserve similar regulatory functions. (3) Peak 4 contains a peptide fragment that is phosphorylated at Ser[503]. Ser[503] is adjacent to the activation loop phosphorylation site in the kinase domain of human PKCδ (NIFGES[503]RAST[507]); its significance is uncertain, since it is not conserved in mouse PKCδ (NIFGEG[501]RAST[505]) or rat PKCδ (NIFGEN[501]RAST[505]). (4) Peak 5 contains peptide fragments phosphorylated at three hinge region residues, Thr[295], Ser[302], and Ser[304].

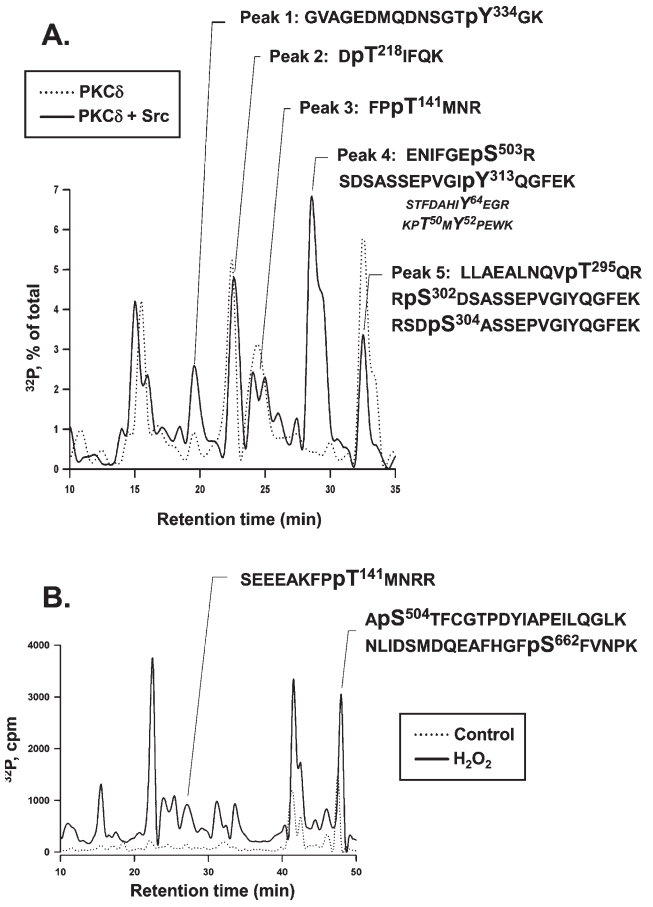

FIGURE 2: PKCδ autophosphorylation at Thr[141], Thr[218], Thr[295], Ser[302], Ser[304], and Ser[503]. Panel A: PKCδ was incubated in a kinase buffer containing [γ-^{32}P]ATP without and with active Src, and PKCδ phosphorylation was tracked by an ESI-LC/MS/MS analysis according to Experimental Procedures. Panel B: Cardiomyocyte cultures were metabolically labeled with ^{32}P and then treated for 10 min with vehicle or 5 mM H_2O_2. Heterologously overexpressed mouse PKCδ was immunoprecipitated from the cultures and then subjected to phosphopeptide mapping analysis as described in Experimental Procedures.

Table 1 provides a summary of the PKCδ autophosphorylation sites detected in these experiments. Several aspects of the results deserve comment. First, the S[302]DS[304]ASSEPVGIY[313]QGFEK peptide fragment was recovered in three separate phosphopeptide mapping experiments as a serine-phosphorylated peptide in peak 5 or as a tyrosine-phosphorylated peptide in peak 4. In each case, the monophosphorylated peptide was detected; we never recovered a dually Ser/Tyr phosphorylated peptide. We also never recovered a dually Ser[302]/Ser[304]-phosphorylated peptide. Second, we detected PKCδ phosphorylation at the turn motif (Ser[645]), but the trypsin digest failed to yield peptides containing either the activation loop (Thr[505]) or hydrophobic motif (Ser[662]) phosphorylation sites. While these phosphorylation reactions are readily detected by immunoblot analysis, these regions of PKCδ were not captured by our sequencing methods that achieved only ~40% coverage of the PKCδ sequence. Other PKCδ autophosphorylation sites may also have evaded detection and deserve further analysis. Third, PKCδ autophosphorylation at Thr[295] and Ser[304] was detected in kinase assays both without and with Src. These results indicate that PKCδ-Tyr[313]/Tyr[334] phosphorylation by Src is not required for PKCδ autophosphorylation at these sites. In contrast, PKCδ autophosphorylation at Thr[141], Thr[218], Ser[503], and Ser[645] was detected exclusively in kinase assays with Src. The significance of this finding is uncertain. Our previous studies using immunoblot analysis showed that Src increases PKCδ autophosphorylation at Thr[505] and Thr[645] (ref *14* and data not shown). Therefore, an effect of Src to increase PKCδ-Thr[505] autophosphorylation might lead to a general increase in PKCδ autophosphorylation

Table 1: Summary of Phosphopeptides Derived from PKCδ Detected by ESI-LC/MS/MS Analysis from *in Vitro* Kinase Assays with PKCδ Alone or PKCδ plus Src[a]

site	phosphopeptide sequence	detected in assays with PMA	detected in assays with PMA + SRC
pT[141]	$_{139}$FP**pT[141]**MNR$_{144}$		+
pT[218]	$_{217}$D**pT[218]**IFQK$_{222}$		+
pT[295]	$_{286}$LLAEALNQV**pT[295]**QR$_{297}$	+	+
pS[302]	$_{301}$R**pS[302]**DSASSEPVGIYQGFEK$_{318}$	+	+
	$_{302}$**pS[302]**DSASSEPVGIYQGFEK$_{318}$		
pS[304]	$_{301}$RSD**pS[304]**ASSEPVGIYQGFEK$_{318}$	+	+
	$_{302}$SD**pS[304]**ASSEPVGIYQGFEK$_{318}$		
pY[313]	$_{301}$RSDSASSEPVGI**pY[313]**QGFEK$_{318}$		+
	$_{302}$SDSASSEPVGI**pY[313]**QGFEK$_{318}$		
pY[334]	$_{320}$TGVAGEDMQDNSGT**pY[334]**GK$_{336}$		+
pS[503]	$_{497}$ENIFGE**pS[503]**R$_{504}$		+
pS[645]	$_{641}$KARL**pS[645]**YSDKNLIDSMOXDQ$_{657}$		+

[a] Y[313] in human PKCδ corresponds to Y[311] in the rodent PKCδ sequence.

throughout the protein. Alternatively, the failure to detect certain phosphopeptides in assays without Src may simply result from a bias inherent in the study; sequencing methods were disproportionately applied to peaks derived from assays with PKCδ plus Src (since PKCδ autophosphorylation was identified as a by-product of studies designed to identify sites for Src-dependent PKCδ tyrosine phosphorylation).

As an initial approach to determine whether these novel phosphorylation sites are modified on PKCδ *in vivo*, mouse PKCδ was overexpressed in cardiomyocyte cultures metabolically labeled with ^{32}P and then treated with H_2O_2 (to activate PKCδ and promote Src-dependent PKCδ tyrosine phosphorylation). PKCδ was then immunoprecipitated and subjected to phosphopeptide mapping analysis. A representative RP-HPLC chromatogram depicted in Figure 2B shows that PKCδ is phosphorylated at Thr^{141}, Ser^{504}, and Ser^{662} (the hydrophobic motif) in H_2O_2-treated cardiomyocytes. These studies provide important evidence that PKCδ-Thr^{141} phosphorylation can be detected *in vivo* in cardiomyocytes. The identification of Ser^{504} as a phosphoacceptor site was more surprising, since autophosphorylation at this site was not detected in the *in vitro* kinase assays. Ser^{504} is an evolutionarily conserved phosphorylation site adjacent to the threonine phosphoacceptor site in the activation loops of PKCδ and aPKCs (ζ and λ/ι); cPKCs or other nPKCs do not contain a phosphorylatable residue at this position. While it is interesting to speculate that this serine may play a redundant role with Thr^{505} to structure the catalytic pocket of PKCδ for catalysis, our recent mutagenesis studies suggest otherwise, showing that a single T505A substitution is sufficient to prevent Src-dependent changes in PKCδ substrate specificity. Detailed studies that consider a possible role for Ser^{504} to substitute for Thr^{505} as a modification that regulates PKCδ's substrate specificity are in progress.

Thr^{141} Contributes to the Control of PKCδ Downregulation in Cells. Previous studies implicated autophosphorylations at residues N-terminal to the pseudosubstrate domain of PKCβII in the control of PKCβII activation. Since Thr^{141} maps to a similar position in PKCδ, we used a heterologous overexpression strategy, with GFP-tagged WT-PKCδ and PKCδ constructs harboring nonphosphorylatable alanine or phosphomimetic aspartate substitutions at position 141 to examine whether Thr^{141} phosphorylation plays a similar role to influence PKCδ activation or downregulation. Figure 3A shows that WT-PKCδ, PKCδ-T141A, and PKCδ-T141D expression is similar in resting COS7 cells. WT-PKCδ and PKCδ-T141A are recovered primarily in the cytosolic fraction, but a smaller pool of WT-PKCδ and PKCδ-T141A constitutively localize to the particulate fraction. PKCδ-T141D also is primarily recovered in the cytosolic fraction. However, a 4.2 ± 0.5-fold greater amount of PKCδ-T141D constitutively partitions to the particulate fraction, relative to WT-PKCδ ($n = 5, p < 0.05$). This increase in constitutive PKCδ-T141D partitioning to the particulate fraction is indicative of *in vivo* PKCδ activation. While a reciprocal decrease in PKCδ-T141D recovery in the soluble fraction is not obvious in Figure 3A, this is due to technical issues related to the detection of small differences in PKCδ immunoreactivity in soluble fractions that contain the bulk of the PKCδ immunoreactivity; the predicted differences in soluble PKCδ levels are resolved when protein loading for soluble fractions is decreased 5-fold (data not shown). Additional studies showed that lipid cofactors such as PMA or the cell-permeable DAG analogue diC8 induce a similar complete translocation of all three enzymes from the soluble to the particulate fraction; no PKCδ, PKCδ-T141A, or PKCδ-T141D immunoreactivity remains in the soluble fraction of PMA- or diC8-treated COS7 cells.

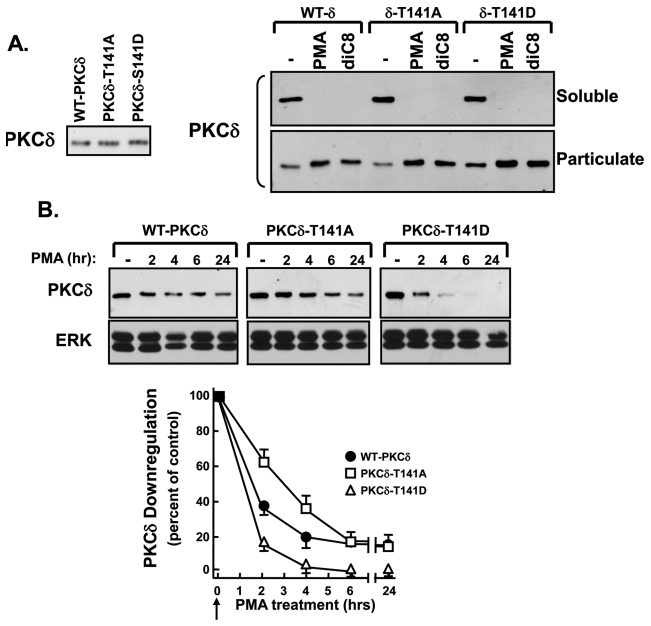

FIGURE 3: An autophosphorylation reaction at Thr^{141} regulates the kinetics of PKCδ activation and downregulation in COS7 cells. Panel A: COS7 cells that heterologously overexpress GFP-tagged WT-PKCδ, PKCδ-T141A, and PKCδ-T141D were treated for 20 min with vehicle, 200 nM PMA, or 200 nM diC8. A small aliquot of cell lysate was retained for Western blotting studies to validate that WT-PKCδ, PKCδ-T141A, and PKCδ-T141D expression levels are similar in resting COS7 cells (left). The remainder of the cell lysate was then partitioned into soluble and particulate fractions according to Experimental Procedures, and then immunoblotting studies were performed to track PKCδ fractionation between soluble and particulate fractions (right). Since PKCδ was expressed as a fusion protein with EGFP, PKCδ was detected with an anti-GFP antibody; no band is identified in uninfected cultures (data not shown). Results are typical of data obtained in five separate experiments. Panel B: COS7 cells that heterologously overexpress WT-PKCδ, PKCδ-T141A, and PKCδ-T141D were treated with vehicle for 24 h or with 200 nM PMA for the indicated intervals; short incubations with PMA were initiated with a delay, so that all samples were harvested simultaneously (and the total treatment interval was similar for all samples). The kinetics of PKCδ protein downregulation was tracked by immunoblot analysis; immunoblotting for ERK is included to control for any minor differences in sample loading. The immunoblotting data and quantification are from a single experiment, with similar results in two separate experiments.

The observation that a T141D substitution leads to the constitutive recruitment of greater amounts of PKCδ to the particulate fraction suggests that a phosphomimetic substitution at Thr^{141} favors PKCδ activation. This conclusion gains support from studies that examine the kinetics of PMA-dependent PKCδ downregulation. While WT-PKCδ, PKCδ-T141A, and PKCδ-T141D were consistently recovered at similar levels under resting culture conditions (arguing that the Thr^{141} substitution does not lead to a gross change in the stability of the enzyme), Figure 3B exposes differences in the kinetics of PKCδ downregulation. PMA treatment leads to a time-dependent decrease in WT-PKCδ abundance; WT-PKCδ abundance falls over the first 4 h of PMA treatment and remains at this reduced level for the next 20 h. While these results are at odds with early studies showing that chronic PMA treatment leads to the complete downregulation of PKCδ, more recent studies with newer lots of anti-PKCδ antibodies (that are considerably more sensitive than the reagents

previously available) indicate that substantial amounts of residual PKCδ immunoreactivity can be detected in various cell types treated with PMA for 24 h. PMA treatment also leads to a time-dependent decline in PKCδ-T141A abundance. However, PMA-dependent PKCδ-T141A downregulation is delayed compared to PMA-dependent downregulation of WT-PKCδ. Of note, residual levels of WT-PKCδ and PKCδ-T141A are similar in COS7 cells treated with PMA for 24 h. In contrast, PMA treatment leads to a considerably more rapid and complete downregulation of PKCδ-T141D. PKCδ-T141D abundance falls dramatically following a 2 h incubation with PMA, and only trace amounts of PKCδ-T141D immunoreactivity are detected in COS7 cells treated with PMA for 4 h; PKCδ-T141D immunoreactivity is not detected in COS7 cells treated with PMA for 24 h. These results are consistent with the notion that a T141A substitution stabilizes the closed conformation of the enzyme and prevents activation/downregulation and that an autophosphorylation (or a negative charge) in the vicinity of the PKCδ pseudosubstrate domain lowers pseudosubstrate domain binding affinity for the catalytic pocket and favors activation.

Thr^{295} Autophosphorylation Regulates in Vitro PKCδ Catalytic Activity. GFP-tagged WT-PKCδ and PKCδ-T295A, and PKCδ-T141A, were overexpressed in COS7 cells and immunoprecipitated for use in kinase assays to determine whether Thr^{295} and Thr^{141} contribute to the control of PKCδ catalytic function. Kinase assays were performed with cTnI as substrate, without and with Src, to determine whether Thr^{295} and Thr^{141} influence PKCδ-Thr^{505} phosphorylation, PKCδ tyrosine phosphorylation by Src, and/or PKCδ phosphorylation of cTnI. Assays also were performed over a range of ATP concentrations to examine whether these phosphorylation sites influence the ATP requirements for PKCδ autophosphorylation or PKCδ phosphorylation of cTnI. Figure 4A shows that WT-PKCδ, PKCδ-T295A, and PKCδ-T141A are recovered as constitutively Thr^{505}-phosphorylated enzymes, indicating that T295A and T141A substitutions do not disrupt *in vivo* PKCδ-Thr^{505} phosphorylation. While we have not yet generated phospho-site-specific antibodies (PSSAs) to track PKCδ phosphorylation at Thr^{295} or Thr^{141}, we noted that Thr^{295} is flanked by a +2 position Arg (i.e., T^{295}QR); the Cell Signaling Technologies anti-pTXR PSSA specifically recognizes this phosphorylation motif. Figure 4 shows that WT-PKCδ and PKCδ-T141A are recovered from COS7 cells without any appreciable anti-pTXR immunoreactivity comigrating with PKCδ. The anti-pTXR PSSA detects *in vitro* WT-PKCδ and PKCδ-T141A autophosphorylation; this autophosphorylation reaction is detected at 1 μM ATP and is maximal at 6 μM ATP. The anti-pTXR PSSA does not detect autophosphorylation of the PKCδ-T295A mutant. The observation that WT-PKCδ and PKCδ-T141A undergo similar *in vitro* autophosphorylation reactions at a site recognized by the anti-pTXR PSSA, whereas the PKCδ-T295A mutant does not, provides strong evidence that the anti-pTXR PSSA specifically recognizes *in vitro* PKCδ autophosphorylation at PKCδ-Thr^{295}. While an effect of the T295A substitution to influence anti-TXR immunoreactivity indirectly by controlling PKCδ autophosphorylation reaction a different TXR motif in PKCδ cannot formally be excluded, other TXR motifs at T^{38}ER and T^{588}KR in human PKCδ have not been identified as autophosphorylation sites; this alternative interpretation of the results is considered substantially less likely. Since the anti-TXR PSSA appears to track PKCδ-Thr^{295} autophosphorylation, it was used to examine whether PKCδ-Thr^{295} autophosphorylation is dynamically regulated

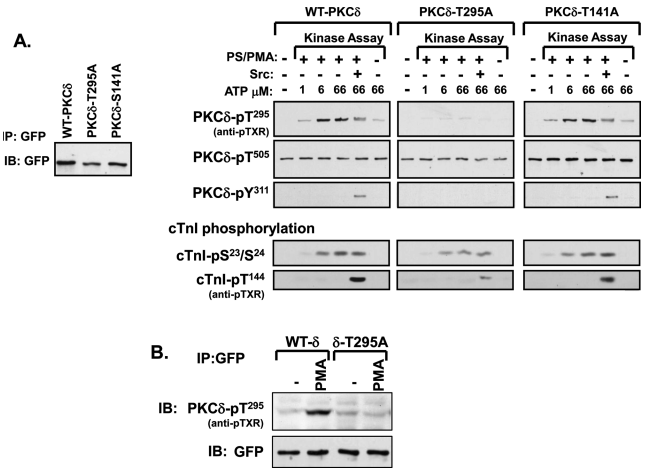

FIGURE 4: PKCδ autophosphorylation at Thr^{295} is required for Src-dependent PKCδ-Tyr^{311} phosphorylation and PKCδ-dependent cTnI phosphorylation at Thr^{144}. Panel A: COS7 cells were transfected with plasmids that drive expression of WT- and T295A- or T141A-substituted forms of PKCδ fused to GFP. PKCδ was immunoprecipitated with anti-GFP and subjected to immunoblotting with anti-GFP to validate equal protein recovery (left). Equal amounts of enzyme were then subjected to immuno-complex kinase assays without and with lipid cofactors, Src, or different ATP concentrations as indicated (right). Immunoblot analysis was used to track PKCδ phosphorylation at Thr^{505}, Thr^{295} (detected with the anti-pTXR PSSA), and Tyr^{311} as well as cTnI phosphorylation at Ser^{23}/Ser^{24} and Thr^{144} (detected with the anti-pTXR PSSA). Panel B: COS7 cells were transfected with plasmids that drive expression of WT-PKCδ or PKCδ-T295A fused to GFP. PKCδ was immunoprecipitated with anti-GFP and subjected to immunoblotting with anti-GFP to validate equal protein recovery (bottom) and anti-TXR immunoreactivity (to track Thr^{295} phosphorylation).

in vivo in COS7 cells. Figure 4B shows that WT-PKCδ and PKCδ-T295A constructs are recovered in similar amounts, without any basal anti-TXR immunoreactivity, from vehicle-treated COS7 cells. The anti-TXR antibody detects a PMA-dependent increase in WT-PKCδ phosphorylation, whereas no PMA-dependent increase in PKCδ-T295A phosphorylation is detected. These results indicate that Thr^{295} phosphorylation also accompanies PKCδ activation *in vivo* in a cellular context.

In vitro kinase assays were performed in the presence of Src, as a strategy to further interrogate the mechanisms that regulate PKCδ activity. Figure 4A shows that WT-PKCδ and PKCδ-T141A are phosphorylated by Src at Tyr^{311} in a similar manner; Src (and PKCδ-Tyr phosphorylation) does not lead to any obvious change in PKCδ autophosphorylation at Thr^{295}. However, the PKCδ-T295A construct (harboring a T → A substitution in the vicinity of Tyr^{311} in the hinge region) shows a relative defect in Src-dependent Tyr^{311} phosphorylation. The functional consequences of altered Thr^{295} autophosphorylation and Src-dependent Tyr^{311} phosphorylation were examined in kinase assays with cTnI as a substrate. cTnI phosphorylation was tracked by immunoblot analysis with an anti-cTnI-pSer^{23}/Ser^{24} PSSA that specifically recognizes the Ser^{23}/Ser^{24}-phosphorylated form of cTnI and the Cell Signaling Technology anti-pTXR PSSA that selectively recognizes cTnI phosphorylation at KRPT^{144}LR (as validated in ref *4*). Allosterically activated forms of WT-PKCδ, PKCδ-T295A, and PKCδ-T141A (in assays with PS/PMA) phosphorylate cTnI at Ser^{23}/Ser^{24} in a similar manner. In each case, cTnI-Ser^{23}/Ser^{24} phosphorylation is detected at 1 μM ATP and maximal at 6 μM ATP. WT-PKCδ and PKCδ-T141A become cTnI-Thr^{144} kinases in assays with Src. Control experiments indicate that cTnI-Thr^{144} phosphorylation

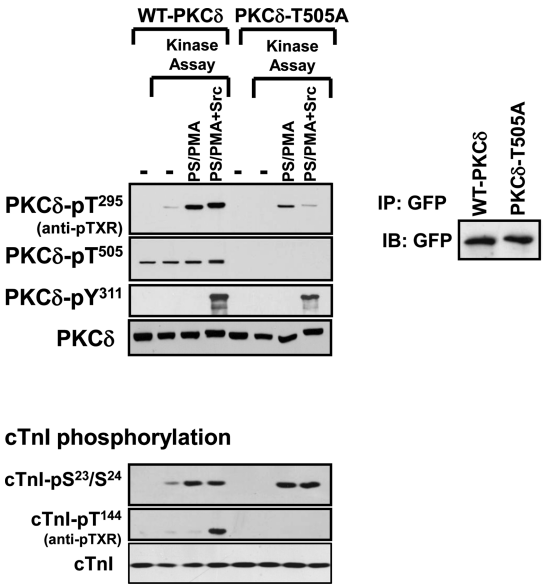

FIGURE 5: The PKCδ-T505A mutant displays a defect in PKCδ autophosphorylation at Thr[295] and PKCδ-dependent cTnI phosphorylation at Thr[144]. Panel A: COS7 cells were transfected with plasmids that drive expression of WT- and T505A-substituted forms of PKCδ fused to GFP. PKCδ was immunoprecipitated with anti-GFP and subjected to immuno-complex kinase assays without and with lipid cofactors or Src (top) and immunoblotting with anti-GFP to validate equal protein recovery (bottom). PKCδ and cTnI phosphorylation were detected as described in the legend to Figure 4. Results were replicated in two additional separate experiments.

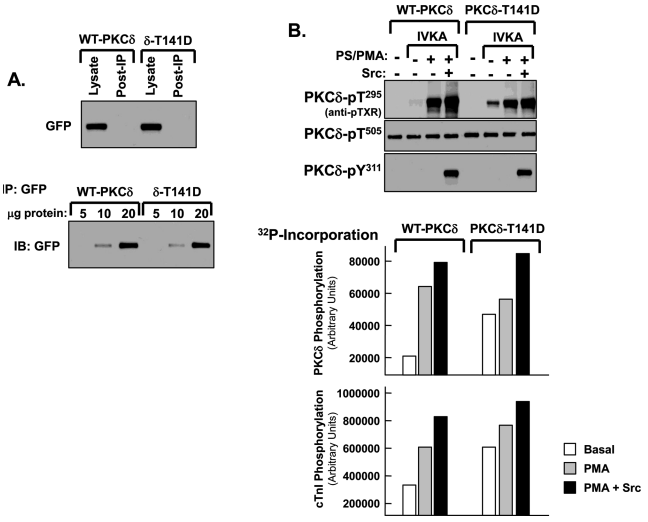

FIGURE 6: A T141D substitution activates PKCδ. COS7 cells were transfected with plasmids that drive expression of WT-PKCδ or PKCδ-T141D fused to GFP; PKCδ was then immunoprecipitated with anti-GFP. Panel A: Immunoblotting of cell lysates to show that WT-PKCδ and PKCδ-T141D expression levels are similar and that the anti-GFP immunoprecipitation protocol clears both enzymes from cell lysates (top). Immunoblotting was performed on increasing amounts of protein recovered in anti-GFP pulldowns to enhance our ability to detect even minor differences in WT-PKCδ versus PKCδ-T141D protein recovery. The Western blot in panel A (bottom) shows that equivalent amounts of WT-PKCδ and PKCδ-T141D were recovered in the anti-GFP pulldowns. Panel B: Equal amounts of WT-PKCδ and PKCδ-T141D were subjected to immuno-complex kinase assays without and with lipid cofactors or Src. Immunoblot analysis was used to track PKCδ phosphorylation at Thr[505], Thr[295] (detected with the anti-pTXR PSSA), and Tyr[311] (top). ^{32}P incorporation into PKCδ and cTnI also was tracked by phosphorimager analysis (bottom). Results are from a single experiment and are representative of three independent experiments with similar results.

cannot be attributed to a contaminant with serine/threonine kinase activity in the Src preparation, since *in vitro* kinase assays with Src and cTnI (without PKCδ) do not lead to any detectable ^{32}P incorporation into cTnI by phosphoimager or evidence of cTnI phosphorylation by immunoblot analysis with the anti-cTnI-Thr[144] PSSA. Of note, a T295A substitution decreases the cTnI-Thr[144] kinase activity of the PKCδ enzyme. These results are consistent with previous studies showing that the effect of Src to convert PKCδ into a cTnI-Thr[144] kinase can be abrogated by a Y311F substitution; the PKCδ-T295A mutant displays a defect in Src-dependent Tyr[311] phosphorylation and decreased cTnI-Thr[144] kinase activity. These results identify a novel PKCδ autophosphorylation reaction at Thr[295] (a highly conserved residue in the hinge region) that is critical for Src-dependent PKCδ-Tyr[311] phosphorylation and consequently Src-dependent changes in PKCδ substrate specificity.

We previously reported that PKCδ acts as a cTnI-Ser[23]/Ser[24] kinase in assays with PS/PMA and as a dual Ser[23]/Ser[24] and Thr[144] kinase in assays with PS/PMA plus Src and that a single T505A substitution prevents the Src-dependent acquisition of cTnI-Thr[144] kinase activity. These studies implicated Thr[505] autophosphorylation as a modification that critically regulates PKCδ phosphorylation of a heterologous substrate. The next set of experiments examined whether Thr[505] phosphorylation regulates PKCδ autophosphorylation at Thr[295]. Figure 5 shows that WT-PKCδ is recovered as a constitutively Thr[505]-phosphorylated enzyme that undergoes an autophosphorylation reaction at Thr[295] in assays performed with PS/PMA. WT-PKCδ phosphorylates cTnI at Ser[23]/Ser[24] in assays with PS/PMA and at Ser[23]/Ser[24] and Thr[144] in assays with PS/PMA and Src. The PKCδ-T505A construct also undergoes an autophosphorylation reaction in assays with PS/PMA (data not shown); PKCδ-T505A phosphorylates cTnI at Ser[23]/Ser[24] in assays with PS/PMA (similar to WT-PKCδ). However, PKCδ-T505A autophosphorylation at Thr[295] and Tyr[311] phosphorylation by Src are defective, relative to WT-PKCδ; Src does not convert the PKCδ-T505A mutant into a cTnI-Thr[144] kinase. Collectively, these results suggest a novel model for PKCδ activation. Our results indicate that PKCδ-Thr[505] autophosphorylation has no effect on some aspects of catalytic activity (for example, cTnI-Ser[23]/Ser[24]), but it is required for optimal PKCδ autophosphorylation at Thr[295] and Src-dependent PKCδ-Tyr[311] phosphorylation, a modification that converts PKCδ into a cTnI-Thr[144] kinase.

A T141D Substitution Favors in Vitro PKCδ Activation. In the final set of experiments, GFP-tagged WT-PKCδ and PKCδ-T141D were overexpressed in COS7 cells and immunoprecipitated for use in kinase assays to determine whether a negative charge at Thr[141] favors PKCδ activation. Figure 6A (top) shows that WT-PKCδ and PKCδ-T141D constructs are expressed at similar levels in COS7 cells and that an immunoprecipitation with an anti-GFP antibody (that recognizes the tag on the heterologously overexpressed PKCδ enzyme) completely clears these enzymes from COS7 cell lysates. Similar amounts of WT-PKCδ and PKCδ-T141D proteins are recovered in anti-GFP pulldowns (Figure 6A, bottom). WT-PKCδ and PKCδ-T141D enzymes were then used in kinase assays without and with PS/PMA (in the absence or presence of Src). Figure 6B shows that WT-PKCδ and PKCδ-T141D are recovered with similar levels of constitutive phosphorylation at Thr[505] but not Thr[295] (i.e., a T141D substitution that increases PKCδ partitioning to the particulate fraction does not lead to an increase in basal

PKCδ-Thr^{295} autophosphorylation in COS7 cells). However, the PKCδ-T141D mutant displays a substantial amount of lipid-independent kinase activity that is not detected in assays with the WT-PKCδ enzyme. PKCδ-T141D executes a robust lipid-independent autophosphorylation reaction, detected as both an increase in Thr^{295} autophosphorylation by immunoblot analysis and an increase in ^{32}P incorporation into the mutant enzyme by phosphorimager analysis. The PKCδ-T141D mutant also is a lipid-independent cTnI kinase. PKCδ-T141D activity is only slightly further increased when assays are performed in the presence of PS/PMA. The Src-dependent increase in Y^{311} phosphorylation is similar for WT-PKCδ and PKCδ-T141D enzymes. These results indicate that a negative charge at Thr^{141} (in the vicinity of the pseudosubstrate domain) disrupts autoinhibitory interactions that restrict basal PKCδ activity.

DISCUSSION

This study identifies seven novel PKCδ autophosphorylation sites in very distinct regions of PKCδ at Thr^{141} adjacent to the pseudosubstrate motif, Thr^{218} in the C1A-C1B interdomain region, Thr^{295}, Ser^{302}, and Ser^{304} in the hinge region, and two serine residues (**S^{501}**RAS**^{504}**T) N-terminal to the activation loop Thr^{505} phosphorylation site. While these novel autophosphorylation sites are evolutionarily conserved in PKCδ, they do not reside in specific phosphorylation motifs common to all PKC isoforms. Rather, these novel autophosphorylation sites map to functionally important regions of the protein that appear to be autophosphorylation "hot spots" in other PKC isoforms. For example, PKCδ and PKCε contain sites for autophosphorylation in the C1A-C1B interdomain region, although the PKCδ C1A-C1B interdomain autophosphorylation site (NSRDT^{218}IF) bears no resemblance to the C1A-C1B interdomain autophosphorylation site recently identified in PKCε (PDQVGS^{234}QR). These results suggest that PKCs may have evolved to contain sites for autophosphorylation at key positions (rather than conserved phosphorylation motifs) in the enzyme. In fact, one could speculate that differences in the autophosphorylation motifs identified in individual nPKC isoforms may have evolved to accommodate the distinct catalytic requirements of these enzymes.

In the course of these studies, two other laboratories identified seven novel sites for PKCδ autophosphorylation at Thr^{50}, Thr^{141}, Ser^{299}, Ser^{302}, Ser^{304}, Thr^{451}, and Ser^{506} (human numbering) (*10*, *15*). Studies from the Parker laboratory suggest that Ser^{299} autophosphorylation may provide a convenient marker for PKCδ activation that could be used (in lieu of more cumbersome methods that assay for PKCδ translocation to membranes) to screen for PKCδ activation in tumor models. The notion that PKCδ autophosphorylation might play a functionally important role to regulate catalysis was not considered. Of the four autophosphorylation sites at Thr^{141}, Ser^{302}, Ser^{304}, and Ser^{506} that were detected in both the previous publication and our study, Thr^{141} is particularly interesting. Thr^{141} is strategically positioned N-terminal to the pseudosubstrate domain, a region that maintains PKCδ in an inactive conformation through an intramolecular interaction with the catalytic pocket. Our mutagenesis studies show that PKCδ is phosphorylated at Thr^{141} *in vivo* in COS7 cells and that Thr^{141} autophosphorylation influences the kinetics of PKCδ activation/downregulation in cells. The PKCδ-T141D mutant is constitutively recovered (in greater amounts than WT-PKCδ) in the particulate fraction; a T141A substitution slows, and a T141D substitution accelerates, the tempo of PKCδ downregulation. *In vitro* kinase assays provide further evidence that a phosphorylation reaction at Thr^{141} relieves autoinhibitory constraints that limit PKCδ activity, showing that the PKCδ-T141D enzyme functions as a lipid-independent serine/threonine kinase. The conclusion that an autophosphorylation at Thr^{141} regulates PKCδ activity resonates with previous modeling studies of PKCβII, which proposed that negative charges due to autophosphorylation reactions at Ser^{16}/Thr^{17} and an Arg residue at position 19 (a position that corresponds to Thr^{141} in PKCδ) participate in intramolecular binding interactions that influence enzyme activity.

Three autophosphorylation sites described in previous studies (at Thr^{50}, Ser^{299}, and Thr^{451}) were not detected in our experiments (although one site was detected in the nonphosphorylated KPT^{50}MY^{52}PEWK peptide fragment, which contains putative phosphorylation sites at both Thr^{50} and Tyr^{52}). Rather, this study identifies novel PKCδ autophosphorylation reactions at Thr^{218} and Thr^{295}, sites not detected in previous studies. Thr^{218} resides in the C1A-C1B interdomain region, within a phosphorylation motif that is conserved in the C1A-C1B interdomain region of PKCθ. Studies of PKCθ implicate this C1A-C1B interdomain autophosphorylation reaction in mechanisms required for proper PKCθ targeting to lipid rafts and antigen receptor signaling responses in Jurkat and T cells (*13*). While the phosphorylation motif detected in PKCδ and PKCθ is not conserved in other PKC isoforms, regulatory autophosphorylation reactions have been identified in the C1A-C1B interdomain regions of PKCε and PKD1 (the founding member of a different family of PMA/DAG-sensitive kinases (*16*)). These results suggest that the C1A-C1B interdomain region may be an autophosphorylation "hot spot" that is exposed on the surface and regulates the localization/actions of these enzymes in cells.

Finally, this study characterizes the variable V3 hinge region of PKCδ as a target for functionally important tyrosine and serine/threonine phosphorylations. We recently reported that Tyr^{311} and Tyr^{332} are the major sites for *in vitro* Src-dependent PKCδ phosphorylation. We also showed that PKCδ is dually phosphorylated at Tyr^{311} and Tyr^{332} in cardiomyocytes subjected to oxidative stress. Recent studies implicate Tyr^{311} phosphorylation as a modification that modulates PKCδ catalytic activity toward Thr^{144} on cTnI. Phosphorylation at Tyr^{332} does not contribute to the control of kinase activity but rather generates a docking site for PKCδ binding partners such as the adapter protein Shc (*17*). Studies reported herein (along with recent results from the Parker laboratory (*10*)) extend the analysis by showing that the human PKCδ hinge region contains a cluster of autophosphorylation sites at Thr^{295}, Ser^{299}, Ser^{302}, and Ser^{304}. These sites, and their flanking sequences, are highly evolutionarily conserved in PKCδ; they are not conserved in other mammalian PKC isoforms (although the hinge regions of PKCβII and PKCε contain their own distinctive autophosphorylation motifs). The Parker laboratory detected PKCδ-Ser^{299} phosphorylation in a dually phosphorylated $_{298}$A**pS^{299}**RR**pS^{302}**DS^{304}ASSEPVGIY^{313}QGFEK^{318} peptide liberated by a 4 h trypsin digest. Ser^{299} phosphorylation was not detected in our experiments that used a lengthier trypsin digestion (16 h), which cleaved the 298−318 peptide fragment into a singly phosphorylated $_{301}$RS^{302}DS^{304}ASSEPVGIY^{313}QGFEK^{318} peptide (with phosphorylation at either Ser^{302}, Ser^{304}, or Tyr^{313}) and a very small $_{298}$ASR^{300} fragment that was not captured in the

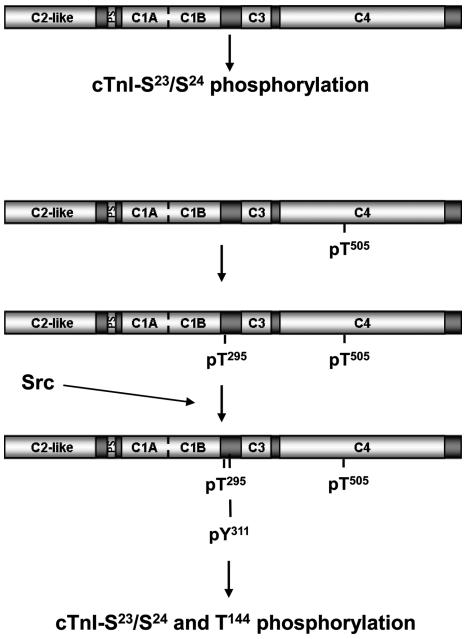

FIGURE 7: Schematic of the controls of PKCδ phosphorylation and activity toward cTnI. See text.

experiments. The Parker laboratory identified a dynamic increase in PKCδ-Ser^{299} phosphorylation in the membrane compartment of PMA-treated COS7 or HeLa cells; a role for PKCδ-Ser^{299} phosphorylation to regulate PKCδ's cellular or *in vitro* catalytic function was not considered. Studies reported herein focused on PKCδ autophosphorylation at Thr^{295}, a different autophosphorylation reaction that was not detected in the previous study. *In vitro* kinase assays exposed a novel role for PKCδ-Thr^{295} autophosphorylation as a lipid-dependent modification that links PKCδ-Thr^{505} autophosphorylation to PKCδ regulation by Src. PKCδ-Thr^{295} autophosphorylation is reduced in the PKCδ-T505A mutant and a T295A substitution leads to a defect in Src-dependent PKCδ-Tyr^{311} phosphorylation. These results provide a molecular explanation for the previous observation that Src phosphorylates PKCδ at Tyr^{311} only when assays are performed in the presence of lipid cofactors. We had previously speculated that lipid cofactors induce a conformational change that renders PKCδ a better substrate for Src. However, studies reported herein expose an additional effect of PMA or DAG to trigger a series of ordered autophosphorylation reactions at Thr^{505} and Thr^{295} that are required for Src-dependent PKCδ-Tyr^{311} phosphorylation (schematized in Figure 7). While a mechanism whereby an autophosphorylation reaction at Thr^{295} would prime PKCδ for subsequent Tyr^{311} phosphorylation by Src is uncertain, these studies suggest that compounds targeted to the PKCδ-Thr^{295} autophosphorylation site might selectively interdict the catalytic function of Tyr^{311}-phosphorylated PKCδ, without acting as general inhibitors of the enzyme. Since there is evidence that the hinge region of PKCβII is exposed (and becomes proteolytically labile) in the active conformation of PKCβII (*8*), the hinge region of PKCδ also is likely to provide an accessible surface for drug interactions. A compound that inhibits PKCδ-Thr^{295} phosphorylation would constitute a novel class of PKCδ inhibitors that would selectively prevent the cellular actions of tyrosine phosphorylated PKCδ (in the soluble fraction of cells exposed to oxidative stress), while preserving PKCδ actions/phosphorylations that result from GPCR activation and the generation of DAG in membranes.

PKC isoforms play key roles in mechanisms that regulate cell proliferation, survival, and migration. PKCs are dysregulated in many clinically important disorders, and genetic studies in PKC knockout models in mice provide compelling evidence that PKC isoforms contribute to the pathogenesis of various immune disorders, atherosclerotic and diabetic cardiovascular diseases, and malignancies. Current methods to screen for PKC activation are quite limited. Most studies have relied on measurements of PKC protein expression, which typically correlates at best only weakly with PKC activation. While measurements of PKC translocation to membranes are more informative, translocation studies are too cumbersome to use as screens for PKC activation (and translocation provides an imperfect measure of enzyme activation under certain circumstances, since some PKCs are activated in the cytosol via nontraditional lipid-independent mechanisms during oxidative stress (*18*)). Studies to determine whether Thr^{295} in PKCδ's hinge region is phosphorylated exclusively via an obligate intramolecular autocatalytic reaction will be critical to determine whether this modification can be exploited as a biomarker to screen for PKCδ activation in biologically relevant tissue samples.

REFERENCES

1. Steinberg, S. F. (2004) Distinctive activation mechanisms and functions for protein kinase C-δ. *Biochem. J. 384*, 449–459.
2. Rybin, V. O., Guo, J., Gertsberg, Z., Feinmark, S. J., and Steinberg, S. F. (2008) Phorbol 12-myristate 13-acetate-dependent protein kinase C-δ-Tyr^{311} phosphorylation in cardiomyocyte caveolae. *J. Biol. Chem. 283*, 17777–17788.
3. Newton, A. C. (2004) Diacylglycerol's affair with protein kinase C turns 25. *Trends Pharmacol. Sci. 25*, 175–177.
4. Sumandea, M. P., Rybin, V. O., Hinken, A. C., Wang, C., Kobayashi, T., Harleton, E., Sievert, G., Balke, C. W., Feinmark, S. J., Solaro, R. J., and Steinberg, S. F. (2008) Tyrosine phosphorylation modifies PKCδ-dependent phosphorylation of cardiac troponin I. *J. Biol. Chem. 283*, 22680–22689.
5. Newton, A. C., and Koshland, D. E.Jr. (1987) Protein kinase C autophosphorylates by an intrapeptide reaction. *J. Biol. Chem. 262*, 10185–10188.
6. Flint, A. J., Paladini, R. D., and Koshland, D. E.Jr. (1990) Autophosphorylation of protein kinase C at three separated regions of its primary sequence. *Science 249*, 408–411.
7. Tsutakawa, S. E., Medzihradszky, K. F., Flint, A. J., Burlingame, A. L., and Koshland, D. E.Jr. (1995) Determination of in vivo phosphorylation sites in protein kinase C. *J. Biol. Chem. 270*, 26807–26812.
8. Orr, J. W., and Newton, A. C. (1994) Intrapeptide regulation of protein kinase C. *J. Biol. Chem. 269*, 8383–8387.
9. Durgan, J., Cameron, A. J., Saurin, A. T., Hanrahan, S., Totty, N., Messing, R. O., and Parker, P. J. (2008) The identification and characterization of novel PKCε phosphorylation sites provides evidence for functional cross-talk within the PKC superfamily. *Biochem. J. 411*, 319–331.
10. Durgan, J., Michael, N., Totty, N., and Parker, P. J. (2007) Novel phosphorylation site markers of protein kinase C-δ activation. *FEBS Lett. 581*, 3377–3381.
11. Rybin, V. O., Guo, J., Sabri, A., Elouardighi, H., Schaefer, E., and Steinberg, S. F. (2004) Stimulus-specific differences in protein kinase C-δ localization and activation mechanisms in cardiomyocytes. *J. Biol. Chem. 279*, 19350–19361.
12. Huang, X., Pi, Y., Lee, K. J., Henkel, A. S., Gregg, R. G., Powers, P. A., and Walker, J. W. (1999) Cardiac troponin I gene knockout: a mouse model of myocardial troponin I deficiency. *Circ. Res. 84*, 1–8.
13. Thuille, N., Heit, I., Fresser, F., Krumbock, N., Bauer, B., Leuthaeusser, S., Dammeier, S., Graham, C., Copeland, T. D., Shaw, S., and Baier, G. (2005) Critical role of novel Thr-219 autophosphorylation for the cellular function of PKCθ in T lymphocytes. *EMBO J. 24*, 3869–3880.
14. Rybin, V. O., Guo, J., Gertsberg, Z., Elouardighi, H., and Steinberg, S. F. (2007) Protein kinase Cε and Src control PKCδ activation loop phosphorylation in cardiomyocytes. *J. Biol. Chem. 282*, 23631–23638.
15. Welman, A., Griffiths, J. R., Whetton, A. D., and Dive, C. (2007) Protein kinase C-δ is phosphorylated on five novel Ser/Thr sites

following inducible overexpression in human colorectal cancer cells. *Protein Sci. 16*, 2711–2715.
16. Hausser, A., Storz, P., Link, G., Stoll, H., Liu, Y. C., Altman, A., Pfizenmaier, K., and Johannes, F. J. (1999) Protein kinase Cμ is negatively regulated by 14-3-3 signal transduction proteins. *J. Biol. Chem. 274*, 9258–9264.
17. Leitges, M., Gimborn, K., Elis, W., Kalesnikoff, J., Hughes, M. R., Krystal, G., and Huber, M. (2002) Protein kinase C-δ is a negative regulator of antigen-induced mast cell degranulation. *Mol. Cell. Biol. 22*, 3970–3980.
18. Steinberg, S. F. (2008) Structural basis of protein kinase C isoform function. *Physiol. Rev. 88*, 1341–1378.